



Electrical and Thermal Conductivity of Ge/Si Quantum Dot Superlattices

Y. Bao,^a W. L. Liu,^a M. Shamsa,^a K. Alim,^a A. A. Balandin,^{a,*} and J. L. Liu^b

^aNano-Device Laboratory, Department of Electrical Engineering, ^bQuantum Structure Laboratory, Department of Electrical Engineering, University of California-Riverside, Riverside, California 92521, USA

Recently proposed thermoelectric applications of quantum dot superlattices made of different material systems depend crucially on the values of the electrical and thermal conductivities in these nanostructures. We report results of the measurements of Hall mobility and thermal conductivity in a set of Ge_{0.5}Si_{0.5}/Si quantum dot superlattices. The average measured in-plane Hall mobility for the undoped Ge/Si quantum dot superlattices on a p-type substrate is 233.5 cm² V⁻¹ s⁻¹ at room temperature and 6.80 × 10³ cm² V⁻¹ s⁻¹ at 77 K. The average value of the thermal conductivity measured by 3ω method is about 10 W/mK at room temperature and 3.5 W/mK at 77 K. In the low-temperature region, the thermal conductivity is proportional to T^{0.7} - T^{0.9}. Relatively large values of the carrier mobility and its temperature dependence suggest that the carrier transport in the investigated structures is likely of the band conduction type rather than hopping type. The thermal conductivity of the Ge_{0.5}Si_{0.5}/Si quantum dot superlattices is strongly reduced and has its peak value shifted toward the high temperatures as compared to the constituent bulk materials. Obtained results can be used for Ge_xSi_{1-x}/Si quantum dot superlattice structure optimization for the high-temperature thermoelectric applications.

© 2005 The Electrochemical Society. [DOI: 10.1149/1.1897365] All rights reserved.

Manuscript received December 2, 2004. Available electronically April 22, 2005.

Quantum dots and different types of quantum dot arrays continue to attract significant attention of the physics and device research communities.¹ Quantum dot superlattices (QDS) have been proposed for the thermoelectric, photodetector, and photovoltaic applications.¹⁻⁵ In all of the envisioned applications, it is crucial to maintain relatively high carrier mobility or product of the mobility and carrier concentration. Good carrier mobility and electric conductivity are important for thermoelectric materials where the figure of merit Z at given temperature T is defined as $ZT = \alpha^2 \sigma T / K$ (where α is Seebeck coefficient, σ is electrical conductivity, and K is thermal conductivity). It is also beneficial for thermoelectric applications to have the lowest possible thermal conductivity. Carrier transport in quantum dot arrays can manifest both hopping transport and conduction band transport features.⁶ The hopping transport regime is characterized by much lower mobility values than the band conduction transport, and by different temperature dependence. What transport regime would prevail depends on the structural and morphological properties of QDS. Despite its importance for practical applications, there has been relatively little work done on carrier transport in QDS.⁷ Experimental investigation of thermal transport in such structures has also just begun. For thermoelectric applications, it is important to measure both electrical and thermal conductivities in the same set of the quantum dot superlattice samples.

In this paper, we report results of measurements of Hall mobility and thermal conductivity in a set of Ge_xSi_{1-x}/Si QDS grown by molecular beam epitaxy (MBE).⁸⁻¹⁰

Sample Description

For this study we have used a batch of MBE grown QDS samples with typical Ge content in the dots of 50%. The investigated QDS had either 5 or 20 layers of quantum dots grown on p-type Si wafers (see Fig. 1). The Ge/Si QDS samples used in this study were fabricated using a solid-source MBE system. P-type (100) Si with a resistivity of 8-10 Ω cm was used as a substrate and cleaned using a standard Shiraki clearing method followed by *in situ* thermal cleaning at 930°C for 15 min. The substrate temperature was maintained at 550°C during the epitaxial growth. The nominal growth rates were 1 and 0.05 Å/s for Si and Ge, respectively. Figure 2a shows a scanning electron microscopy (SEM) image of the top layer of the undoped Ge/Si quantum dot samples. The Ge dots can be seen as bright disks. From this SEM image, we can determine some characteristics of the quantum dot array. We estimated that the density of Ge quantum dots is about 3 × 10⁹ cm⁻² and the average base diam-

eter is 40 nm. The height of 4 nm has been determined from the atomic force microscopy scans.

Thermally diffused contacts made of aluminum were formed on top of the superlattices to carry out Hall measurements (Fig. 2b). Extended annealing time has been chosen to make sure that the contact is formed for all layers of quantum dots. The voltage was applied across the gap between the pairs of electrodes, so that current flows parallel to the quantum dot layers. Before measuring the carrier mobility we have verified that the electrical contacts are indeed Ohmic by carrying out IV measurements between different pairs of electrodes and switching the polarity. It has been established that in the examined range of biases from -2 V to +2 V the electrical current varies from -0.02 A to +0.02 A, and it depends strictly linearly on the applied bias voltage.

From the data obtained by micro-Raman spectroscopy we have established that the Ge dot layers were not under very strong strain. This conclusion is based on comparison of Si and Ge peak positions in Ge/Si QDS with those in bulk Si (520.4 cm⁻¹) and Ge (301 cm⁻¹). Raman spectroscopy has been carried out using Renishaw instrument under 488 nm laser excitation. Figure 3 shows typical spectra for two samples. The position of TO peak in Ge dots and bulk Si are indicated by the arrows. In some QDS samples, the peak position coincides with bulk almost exactly. The spectra of undoped samples LJ017 and LJ018 shown in Fig. 3 exhibit only small deviation.

Hall Mobility Measurements

The Hall mobility was measured using EGK HEM-2000 system at the room temperature and 77 K. The measurements were conducted in a standard four-terminal scheme to ensure the accuracy. The data points were taken at the magnetic field of 0.37 T. In Fig. 4, we present Hall mobility Ge/Si quantum dot superlattices at room temperature and 77 K. The Hall mobility μ_H is shown as a function of input current I_{inp} to demonstrate its weak dependence on I_{inp} . The Hall mobility μ_H is defined as the product of the Hall coefficient R_H and the electric conductivity σ

$$\mu_H = |R_H \sigma| \quad [1]$$

where $R_H = (p - nb^2) / e(p + nb)^2$, and $b = \frac{\mu_e}{\mu_h}$ is the ratio of the electron μ_e and hole μ_h drift mobilities, $n(p)$ is the electron (hole) density, and e is the charge of an electron. The Hall mobility can be readily correlated with the electron or hole mobility for the heavily doped samples where $n \gg p$ (or $p \gg n$). In the general case, the Hall mobility is related to the drift mobility (one type of carriers) through the expression $\mu_H = \langle \langle \tau^2 \rangle \rangle / \langle \langle \tau \rangle \rangle^2 \mu_{drift}$.¹¹ Here τ is the scat-

* Electrochemical Society Active Member.

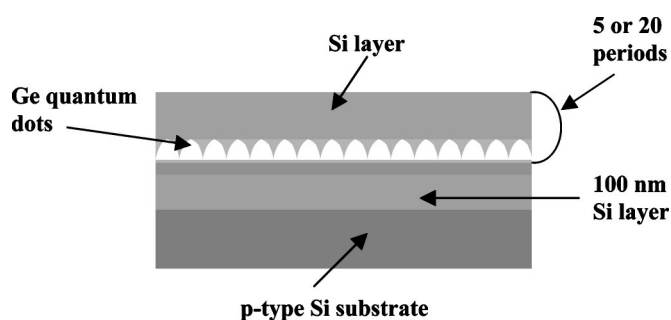
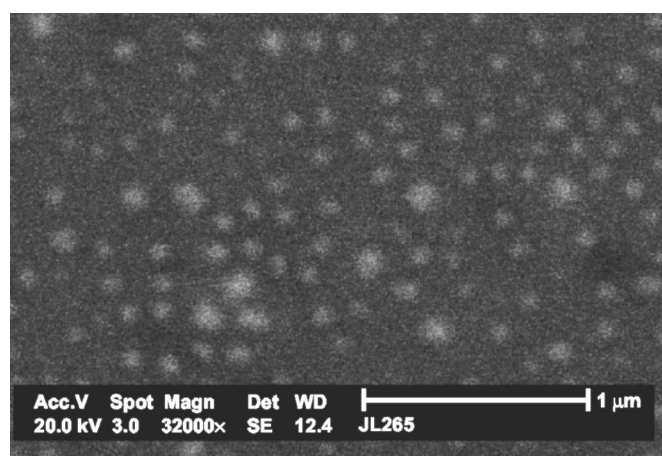
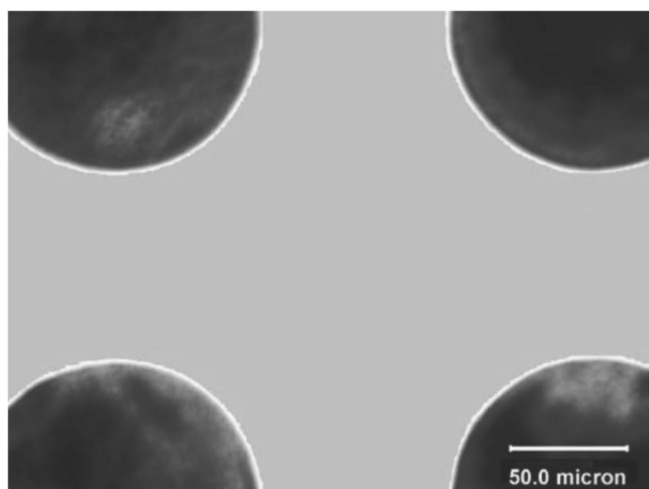


Figure 1. Schematic of the quantum dot superlattices structure.



(a)



(b)

Figure 2. (a) SEM image of Ge quantum dots on Si grown by molecular beam epitaxy. (b) Optical micrograph of the electrodes on a sample.

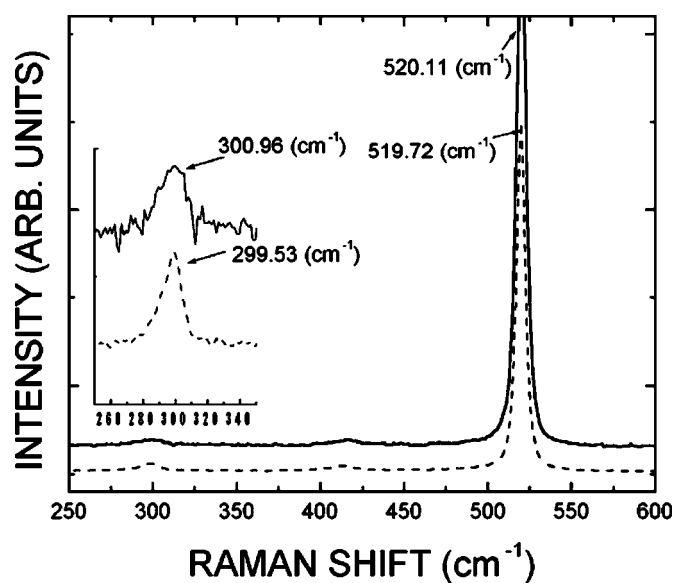


Figure 3. Raman spectra of Ge/Si quantum dot superlattices taken under 488 nm excitation at room temperature.

tering time, the symbol $\langle\langle\rangle\rangle$ denotes averaging for the relaxation time defined as $\langle\langle\tau\rangle\rangle = \langle E\tau\rangle/\langle E\rangle$, where E is the energy of the carrier and symbol $\langle\rangle$ denotes standard ensemble average. The measured values of the Hall coefficient were positive indicating the overall p-type conduction. Table I summarizes the average measured values of the Hall mobility and apparent carrier concentration for the investigated quantum dot superlattices. For comparison, the room temperature electron (hole) drift mobility in bulk Si and Ge are $\mu_e = 1500 \text{ cm}^2 \text{ V}^{-1} \text{ s}^{-1}$ ($\mu_p = 450 \text{ cm}^2 \text{ V}^{-1} \text{ s}^{-1}$) and $\mu_e = 3900 \text{ cm}^2 \text{ V}^{-1} \text{ s}^{-1}$ ($\mu_p = 1900 \text{ cm}^2 \text{ V}^{-1} \text{ s}^{-1}$), respectively. Electron (hole) drift mobility at 77 K can be estimated from the equation $\mu = \mu_0(T/T_0)^{-3/2}$, where $T_0 = 300 \text{ K}$ and μ_0 is the drift mobility at $T = 300 \text{ K}$.¹² Thus, at 77 K one gets $\mu_e = 3.0 \times 10^4 \text{ cm}^2 \text{ V}^{-1} \text{ s}^{-1}$, $\mu_p = 1.5 \times 10^4 \text{ cm}^2 \text{ V}^{-1} \text{ s}^{-1}$ for intrinsic Si and $\mu_e = 1.2 \times 10^4 \text{ cm}^2 \text{ V}^{-1} \text{ s}^{-1}$, $\mu_p = 3.5 \times 10^3 \text{ cm}^2 \text{ V}^{-1} \text{ s}^{-1}$ for intrinsic Ge. Using Eq. 1 and the formula for the Hall coefficient, we can also estimate what should be the Hall mobility for intrinsic Si and Ge. At

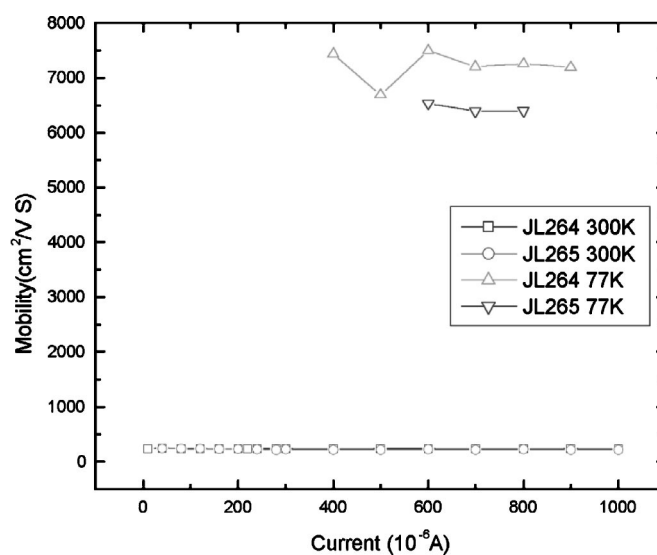


Figure 4. Hall mobility μ_H in Ge/Si quantum dot superlattice at room temperature and at 77 K.

Table I. Hall mobility in Ge/Si quantum dots superlattices

Quantum superlattices	DOT 300 K μ_H (cm ² /Vs)	N_b (cm ⁻³)	77 K μ_H (cm ² /Vs)	N_b (cm ⁻³)
Ge/Si QDS (JL264 undoped N = 5)	239	7.57×10^{18}	7.2×10^3	2.86×10^{18}
Ge/Si QDS (JL265 undoped N = 20)	228	1.76×10^{18}	6.4×10^3	7.98×10^{17}

room temperature, the intrinsic Si carrier densities are $n = p = n_i = 1.5 \times 10^{10} \text{ cm}^{-3}$, and the electron and hole drift mobilities are $\mu_e = 1500 \text{ cm}^2 \text{ V}^{-1} \text{ s}^{-1}$ and $\mu_p = 450 \text{ cm}^2 \text{ V}^{-1} \text{ s}^{-1}$, correspondingly. Thus, one can estimate the Hall mobility to be $1050 \text{ cm}^2 \text{ V}^{-1} \text{ s}^{-1}$. Analogously, for intrinsic Ge, $n = p = n_i = 2.4 \times 10^{13} \text{ cm}^{-3}$, and the electron and hole drift mobilities are $\mu_e = 3900 \text{ cm}^2 \text{ V}^{-1} \text{ s}^{-1}$, $\mu_p = 1900 \text{ cm}^2 \text{ V}^{-1} \text{ s}^{-1}$. Thus, the Hall mobility for Ge is $2000 \text{ cm}^2 \text{ V}^{-1} \text{ s}^{-1}$. The calculated Hall mobility μ_H at 77 K for intrinsic Si and Ge is $1.5 \times 10^4 \text{ cm}^2 \text{ V}^{-1} \text{ s}^{-1}$ and $8 \times 10^3 \text{ cm}^2 \text{ V}^{-1} \text{ s}^{-1}$, respectively.

As can be seen from Table I, the average value for the undoped QDS is $233.5 \text{ cm}^2 \text{ V}^{-1} \text{ s}^{-1}$ at room temperature, and $6.80 \times 10^3 \text{ cm}^2 \text{ V}^{-1} \text{ s}^{-1}$ at 77 K. These values are much less than those for Si and Ge Hall mobilities. At the same time the QDS Hall mobility values are larger than typical mobility values in the hopping conduction regime. The decrease of the Hall mobility in QDS compared to the bulk intrinsic value can be attributed to the presence of the potential barriers at the Ge/Si interface, charging effects, surface disorder, and alloy scattering, etc. Moreover, most of the band discontinuity between Ge and Si resides in the valence band thus stronger impeding the hole transport. A study of the dislocation line density conducted for the samples grown by the same group¹³ indicates that the high-density dislocations are generated when the number of layers is larger than 25. Thus, in the investigated QDS samples the role of the dislocation lines on the carrier transport is not expected to be strong. One can also note from Table I and Fig. 4, that the Hall mobility at 300 K is much smaller than that at 77 K, which is characteristic for the band conduction-type transport. Indeed, in conventional semiconductors, mobility increases with decreasing temperature (from 300 to 77 K) due to reduction in phonon scattering.^{11,12} In the hopping transport regime, characteristic for disordered systems, the temperature dependence of the mobility is different. This regime is sometimes observed in quantum dot arrays^{6,14} or nanoparticle samples. Under the assumption of conventional phonon-assisted hopping transport regime the conductance in quantum dot array is described by the equation¹⁴ $G(T) = G_0 \exp\{- (T_0/T)^x\}$, where T_0 is a parameter determined by the properties of the material, and parameter $x < 1$ is defined by the energy dependence of the density of states near the Fermi level. In the case when the interaction energy between electron and a hole is large compared to energy perturbation due to disorder, parameter $x = 1/2$, and the conductivity is described by the Efros-Shklovskii law.¹⁵ In the hopping transport regime, the mobility is higher and, correspondingly, the resistivity is lower, at high temperature than at low temperature due to the temperature activation mechanism. Results of our measurements suggest that for given Ge/Si quantum dot superlattices the carrier transport is of the band type rather than thermally activated hopping type.¹⁴⁻¹⁶

Thermal Conductivity Measurements

The thermal conductivity of the QDS was measured in the extended temperature range from 10 to 400 K using a home-built 3ω experimental setup. Details of the 3ω -measurement technique can be found in Ref. 17. On the top surface of the samples, we deposited SiN_x layer with the thickness of 100 nm using the plasma-enhanced chemical vapor deposition (PECVD). This layer was required to provide electrical insulation for the measurement. The Cr (100 Å)/Au (1000 Å) metallic 3ω heater-thermometer with the wire width of 5 μm was patterned on the insulation layer and fabricated by e-beam evaporation and lift-off technique. Figure 5a

shows the top view of the fabricated 3ω heater. To facilitate the differential measurements, a Si reference sample used to measure the thermal conductivity of the insulation layer and substrate, was prepared and also coated with PECVD SiN_x and pattern with the 3ω -heater-thermometer. The 3ω measurements were conducted inside a vacuum cryostat in the temperature range from 10 to 400 K. An SR850 lock-in amplifier was used to provide first harmonic input power and collect the third harmonic temperature-rise signals from

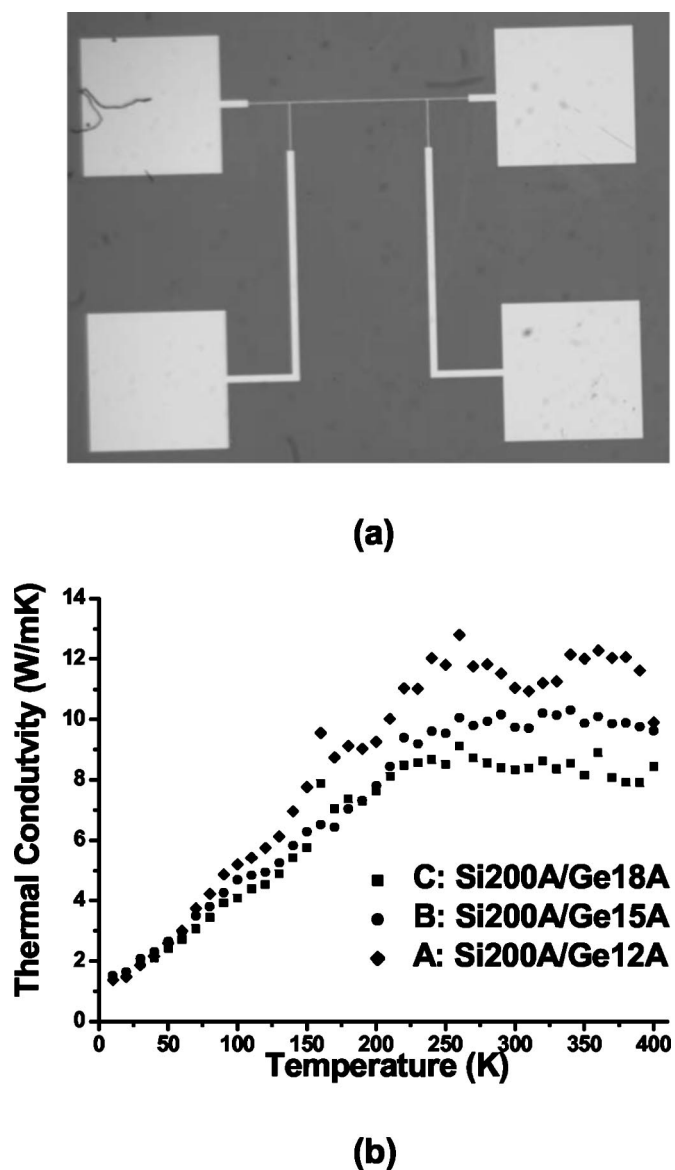


Figure 5. (a) Top view micrograph of the heater-thermometer fabricated for the thermal conductivity measurements by the 3ω technique. (b) Measured temperature dependence of the thermal conductivity for three Ge/Si quantum dot superlattices.

the sample. A numerical program based on the analytical solution of the 3ω heat conduction model was developed to fit the experimental data and obtained the thermal conductivity.

Figure 5b shows the measured thermal conductivity as a function of temperature for three QDS samples. The bilayer thicknesses of the samples are indicated in the figure legend. The measured data indicate significant reduction of the cross-plane thermal conductivity compare to bulk constituent materials. The peak thermal conductivity values of the measured samples are shift to higher temperatures (near room temperature). In bulk crystalline semiconductors such as Si or Ge, the maximum value is achieved around 20 K. The observed shift of the maximum value is in line with reported data.¹⁸ The average thermal conductivity of the three samples is about 10 W/mK at 300 K and 3.5 W/mK at 77 K. Another important observation is that in the low-temperature region, the thermal conductivity is proportional to $T^{0.7} - T^{0.9}$. This temperature dependence differs significantly from that one in bulk materials. The strongly reduced thermal conductivity with relatively good electrical conductivity of Ge/Si QDS indicate that such structures are promising candidates for thermoelectric applications.^{19,20}

Note that the examined QDS were characterized by only partial ordering of quantum dots (vertical site correlation). Further improvement in the growth technique is expected to lead to three-dimensional (3D) regimentation of quantum dots, with corresponding modification of the electron and phonon dispersion.²¹ The latter would allow a better control of the electrical and thermal transport in QDS. Tuning of the phonon transport, *i.e.*, phonon engineering, may lead to additional reduction of the thermal conductivity and enhancement of the thermoelectric figure of merit of QDS.

Conclusions

For the proposed thermoelectric applications of quantum dot superlattices it is important to understand the specifics of both electrical and thermal conduction in such nanostructures. In this paper, we report results of the measurements of Hall mobility and thermal conductivity in a set of $\text{Ge}_{0.5}\text{Si}_{0.5}/\text{Si}$ quantum dot superlattices. The average measured in-plane Hall mobility for the undoped Ge/Si quantum dot superlattices on p-type substrate is $233.5 \text{ cm}^2 \text{ V}^{-1} \text{ s}^{-1}$ at room temperature and $6.80 \times 10^3 \text{ cm}^2 \text{ V}^{-1} \text{ s}^{-1}$ at 77 K. The average value of the thermal conductivity measured by 3ω method is about 10 W/mK at 300 K and 3.5 W/mK at 77 K. In the low-temperature region, the thermal conductivity is proportional to $T^{0.7} - T^{0.9}$. Relatively large values of the charge carrier mobility

and significantly reduced thermal conductivity indicate that the examined structures are good candidates for the “electron transmitting-phonon blocking” structures required for thermoelectric applications.

Acknowledgement

The work in the Nano-Device Laboratory (<http://ndl.ee.ucr.edu/>) has been supported in part by the National Science Foundation and DARPA/DMEA CNID center.

The University of California at Riverside assisted in meeting the publication costs of this article.

References

1. K. L. Wang and A. A. Balandin, in *Optics of Nanostructured Materials*, V. Markel and T. George, Editors, p. 515, John Wiley & Sons, New York (2001).
2. (a) A. A. Balandin and O. L. Lazarenkova, *Appl. Phys. Lett.*, **82**, 415 (2003); (b) O. L. Lazarenkova and A. A. Balandin, *J. Appl. Phys.*, **89**, 5509 (2001).
3. T. C. Harman, P. J. Taylor, D. L. Spears, and M. P. Walsh, *J. Electron. Mater.*, **29**, 11 (2000).
4. (a) V. A. Fonoberov and E. P. Pokatilov, *Phys. Rev. B*, **66**, 085310 (2002); (b) S. Tong, J. L. Liu, J. Wan, and K. L. Wang, *Appl. Phys. Lett.*, **80**, 1189 (2003).
5. E. Towe and D. Pan, *IEEE J. Sel. Top. Quantum Electron.*, **6**, 408 (2001).
6. H. Z. Song, K. Akahane, S. Lan, H. Z. Xu, Y. Okada, and M. Kawabe, *Phys. Rev. B*, **64**, 085303 (2001).
7. (a) A. I. Yakimov, C. J. Adkins, R. Boucher, A. V. Dvurechenskii, A. I. Nikiforov, O. P. Pchelyakov, and G. Biskupski, *Phys. Rev. B*, **59**, 12598 (1999); (b) A. I. Yakimov, A. V. Dvurechenskii, A. I. Nikiforov, and A. A. Bloshkin, *JETP Lett.*, **77**, 376 (2003).
8. J. L. Liu, W. G. Wu, A. A. Balandin, G. Jin, and K. L. Wang, *Appl. Phys. Lett.*, **74**, 185 (1999).
9. Y. H. Xie, S. B. Samavedam, M. Bulsara, T. A. Langdo, and E. A. Fitzgerald, *Appl. Phys. Lett.*, **71**, 3567 (1997).
10. V. Ya. Aleshkin, N. A. Bekin, N. G. Kalugin, Z. F. Krasilnik, A. V. Novikov, V. V. Postnikov, and H. Seyringer, *JETP Lett.*, **67**, 48 (1998).
11. J. Singh, *Physics of Semiconductors and Their Heterostructures*, McGraw-Hill, New York (1993).
12. S. M. Sze, *Semiconductor Devices: Physics and Technology*, Wiley, New York (1985).
13. J. L. Liu, J. Wan, K. L. Wang, and D. P. Yu, *J. Cryst. Growth*, **251**, 666 (2003).
14. (a) A. I. Yakimov, A. V. Dvurechenskii, A. I. Nikiforov, and A. A. Bloshkin, *JETP Lett.*, **77**, 376 (2003); (b) A. I. Yakimov, A. V. Dvurechenskii, A. I. Nikiforov, and C. J. Adkins, *Phys. Status Solidi B*, **218**, 99 (2000).
15. A. L. Efros and B. I. Shklovskii, *J. Phys. C*, **8**, L49 (1975).
16. M. Furlan, *Phys. Rev. B*, **57**, 14818 (1998).
17. D. G. Cahill, *Rev. Sci. Instrum.*, **61**, 802 (1990).
18. W. L. Liu, T. Borca-Tasciuc, G. Chen, J. L. Liu, and K. L. Wang, *J. Nanosci. Nanotechnol.*, **1**, 39 (2001).
19. J. Zou and A. A. Balandin, *J. Appl. Phys.*, **89**, 2932 (2001).
20. Y. Bao, A. A. Balandin, J. L. Liu, J. Liu, and Y. H. Xie, *Appl. Phys. Lett.*, **84**, 3355 (2004).
21. O. L. Lazarenkova and A. A. Balandin, *Phys. Rev. B*, **66**, 245319 (2002).